

Reliability-output Decoding of Tail-biting Codes

Adam R. Williamson, *Student Member, IEEE*, Matthew Marshall, and Richard D. Wesel, *Senior Member, IEEE*

Abstract—We present an extension to Raghavan and Baum’s reliability-output Viterbi algorithm (ROVA) to accommodate tail-biting convolutional codes. This tail-biting ROVA computes the exact word-error probability of the decoded codeword by calculating the posterior probability of tail-biting codeword’s starting state. We then introduce a state-estimation algorithm based on the posterior distribution of the starting states that selects the maximum a posteriori state. An approximation to the exact tail-biting ROVA that estimates the word-error probability is also presented. A comparison of the computational complexity of each approach is discussed in detail. These tail-biting reliability-output algorithms are suitable for use in reliability-based retransmission schemes with short blocklengths, in which terminated convolutional codes would suffer rate loss.

I. INTRODUCTION

Raghavan and Baum’s reliability-output Viterbi algorithm (ROVA) [1] uses the sequence-estimation property of the Viterbi algorithm to calculate the exact word-error probability of a received convolutional code sequence. In general, the ROVA can be used to compute the word-error probability for any finite-state Markov process observed via memoryless channels (i.e., processes with a trellis structure). However, the ROVA is only valid for processes that terminate in a known state (usually the all-zeros state). For codes with large constraint lengths ($\nu + 1$), a significant rate penalty is incurred due to the ν additional symbols that must be transmitted in order to arrive at the termination state.

Tail-biting convolutional codes can start in any state, but must terminate in the same state. The starting/terminating state is unknown at the receiver. These codes do not suffer the rate loss of terminated codes, making them throughput-efficient (see, e.g., [2] and [3, Ch. 12.7]). The tail-biting technique is commonly used for short-blocklength coding.

A. Overview and Contributions

In this paper, we extend the ROVA to compute the word-error probability for tail-biting codes. First, we present a straightforward approach, which we call the tail-biting ROVA (TB ROVA). TB ROVA invokes the original ROVA for each of the possible starting states s . The complexity of this straightforward approach is large, proportional to $2^{2\nu}$ for standard binary convolutional codes (and $q^{2\nu}$ for convolutional codes over Galois field $GF(q)$).

We explore several approaches to reduce the complexity of TB ROVA. We first introduce a post-decoding algorithm that computes the reliability of codewords that have already

been decoded by an existing tail-biting decoder, including possibly suboptimal decoders. We then propose a new tail-biting decoder that uses the posterior distribution of the starting states to identify the most probable starting state of a received sequence. Finally, we discuss how to use Fricke and Hoeher’s simplified (approximate) ROVA [4] for each of the q^ν initial states, which reduces the complexity of the word-error probability computation but not the actual ML decoding complexity.

The remainder of this paper proceeds as follows: Sec. I-B reviews the related literature and Sec. I-C introduces notation. Sec. II reviews Raghavan and Baum’s ROVA and discusses how to extend it to tail-biting codes. Sec. III presents the Post-decoding Reliability Computation (PRC) for tail-biting codes and Sec. IV introduces the Tail-Biting State-Estimation Algorithm (TB SEA). The simplified ROVA for tail-biting codes is discussed in Sec. V. Sec. VI discusses an alternative to TB SEA using the tail-biting BCJR algorithm. Sec. VII evaluates the complexity of the proposed algorithms. Sec. VIII shows numerical examples of the computed word-error probability and the actual word-error probability. Trellis-based reliability-output decoding for linear block codes is discussed briefly in Sec. IX. Sec. X concludes the report.

B. Related Literature

There are a number of reliability-based decoders for terminated convolutional codes, most notably the Yamamoto-Itoh algorithm [5], which computes a reliability measure for the decoded word, but not the exact word-error probability. Fricke and Hoeher [6] use Raghavan and Baum’s ROVA in a reliability-based type-I hybrid ARQ scheme.

Hof et al. [7] modify the Viterbi algorithm to permit generalized decoding according to Forney’s generalized decoding rule [8]. When the generalized decoding threshold is chosen for maximum likelihood (ML) decoding with erasures and the erasure threshold is chosen appropriately, this augmented Viterbi decoder is equivalent to the ROVA.

A type-II hybrid ARQ (incremental redundancy) scheme for punctured terminated convolutional codes is presented by Williamson et al. [9]. In [9], additional coded symbols are requested when the word-error probability computed by the ROVA exceeds a target word-error probability. This word-error requirement facilitates comparisons with recent work in the information theory community [10], [11]. Polyanskiy et al. [11] investigates the maximum rate achievable at short blocklengths with variable-length feedback codes. While [9] shows that terminated convolutional codes can deliver throughput above the random-coding lower bound of [11], the rate loss from termination is still significant at short blocklengths. For this reason, it is imperative to have a reliability-output decoding algorithm for tail-biting codes.

A. R. Williamson, M. Marshall, and R. D. Wesel are with the Electrical Engineering Department, University of California, Los Angeles, CA 90095 USA (e-mail: adamroyce@ucla.edu; mmarshall@ucla.edu; wesel@ee.ucla.edu).

This research was supported by National Science Foundation Grant CIF CCF 1162501.

In contrast to the decoding algorithms for terminated codes, Anderson and Hladik [12] present a tail-biting maximum a posteriori (MAP) decoding algorithm. This extension of the BCJR algorithm [13] can be applied to tail-biting codes with a priori unequal source data probabilities. As with the BCJR algorithm, [12] computes the posterior probabilities of individual data symbols. In contrast, the ROVA [1] and the tail-biting reliability-based decoders in this paper compute the posterior probabilities of the codeword.

More importantly, the tail-biting BCJR of [12] is only an approximate symbol-by-symbol MAP decoder, as pointed out in [14] and [15]. Because the tail-biting restriction is not strictly enforced, non-tail-biting “pseudocodewords” can cause bit errors, especially when the ratio of the tail-biting length L to the memory length ν is small (i.e., $L/\nu \approx 1$ -2). Further comparisons with the tail-biting BCJR are given in Sec. VI. An exact symbol-by-symbol MAP decoder for tail-biting codes is given in [16, Ch. 7].

Handlery et al. [17] introduce a suboptimal, two-phase decoding scheme for tail-biting codes that computes the approximate posterior probabilities of each starting state and then uses the standard BCJR algorithm to compute the posterior probabilities of the source symbols. This approach is compared to the tail-biting BCJR of [12] and exact MAP decoding in terms of bit-error-rate (BER) performance. Both the two-phase approach of [17] and the tail-biting BCJR of [12] perform close to exact MAP decoding when L/ν is large, but suffer a BER performance loss when L/ν is small.

Although it does not compute the word-error probability, Yu [18] introduces a method of estimating the initial state of tail-biting codes, which consists of computing a pre-metric for each state based on the last ν observations of the received word. This pre-metric is then used to initialize the path metrics of the main tail-biting decoder (e.g., the circular Viterbi decoder [19]), instead of assuming that all states are equally likely at initialization. The state-estimation method of [18], which is not maximum-likelihood, is limited to systematic codes and a special configuration of nonsystematic codes that allows information symbols to be recovered from noisy observations of coded symbols.

Because tail-biting codes can be viewed as circular processes [2], [19], decoding can start at any symbol. Wu et al. [20] describe a reliability-based decoding method that compares the log likelihood-ratios of the received symbols in order to determine the most reliable starting-location for tail-biting decoders. Selecting a reliability-based starting-location reduces the error probability by minimizing the chance of choosing non-tail-biting paths early in the decoding process. Wu et al. [20] apply this approach to existing suboptimal decoders, including the wrap-around Viterbi algorithm of [21]. As with [18], [20] does not compute the word-error probability.

Pai et al. [22] generalizes the Yamamoto-Itoh algorithm to handle tail-biting codes and uses the computed reliability measure as the retransmission criteria for hybrid ARQ. When there is a strict constraint on the word-error probability, however, this type of reliability measure is not sufficient to guarantee a particular undetected-error probability. Providing such a

guarantee motivates the word-error probability calculations in this paper (instead of bit-error probability as in [12], [14]–[18]).

C. Notation

We use the following notation in this paper: $P(X = x)$ denotes the probability mass function (p.m.f.) of discrete-valued random variable X at value x , which we also write as $P(x)$. The probability density function (p.d.f.) of a continuous-valued random variable Y at value y is $f(Y = y)$, sometimes written as $f(y)$. In general, capital letters denote random variables and lowercase letters denote their realizations. Superscripts denote vectors unless otherwise noted, as in $y^\ell = (y_1, y_2, \dots, y_\ell)$, while subscripts denote a particular element of a vector: y_i is the i th element of y^ℓ . We use the hat symbol to denote the output of a decoder, e.g., \hat{x} is the codeword chosen by the Viterbi algorithm.

II. THE RELIABILITY-OUTPUT VITERBI ALGORITHM

Raghavan and Baum’s reliability-output Viterbi algorithm [1] augments the canonical Viterbi decoder with the computation of the word-error probability of the maximum-likelihood (ML) codeword. In this section, we provide an overview of the ROVA.

For rate- k/n convolutional codes with L trellis segments and input alphabet q , we denote the ML codeword as $\hat{x}^L = \hat{x}$ and the noisy received sequence as $y^L = y$. The probability that the ML decision is correct given the received word is $P(X = \hat{x}|Y = y) = P(\hat{x}|y)$, and the word-error probability is $P(X \neq \hat{x}|Y = y) = 1 - P(\hat{x}|y)$. The probability of successfully decoding can be expressed as follows:

$$P(\hat{x}|y) = \frac{f(y|\hat{x})P(\hat{x})}{f(y)} = \frac{f(y|\hat{x})P(\hat{x})}{\sum_{x'} f(y|x')P(x')}, \quad (1)$$

where we have used $f(y|\hat{x})$ to denote the conditional p.d.f. of the real-output channel (e.g., the binary-input AWGN channel). This may be replaced by the conditional p.m.f. $P(y|\hat{x})$ for discrete-output channels (e.g., the BSC).

The probability of correctly decoding can be further simplified if each of the codewords x' is a priori equally likely, i.e., $P(\hat{x}) = P(x') \forall x' \neq \hat{x}$, which we assume for the remainder of the paper. This assumption yields

$$P(\hat{x}|y) = \frac{f(y|\hat{x})}{\sum_{x'} f(y|x')}. \quad (2)$$

In general, the denominator in (2) may be computationally intractable when the message set cardinality is large. However, the ROVA [1] takes advantage of the trellis structure of convolutional codes to compute $P(\hat{x}|y)$ exactly with complexity that is linear in the blocklength and exponential in the constraint length of the code (i.e., it has complexity on the same order as that of the original Viterbi algorithm). This probability can also be computed approximately by the simplified (approximate) ROVA [4], which will be discussed further in Sec. V.

The ROVA can compute the probability of word error for any finite-state Markov process observed via memoryless

channels (e.g., in maximum-likelihood sequence estimation for signal processing applications). In the remainder of this paper, we use the example of convolutional encoding and decoding, but the ROVA and our tail-biting trellis algorithms apply to any finite-state Markov process.

A. Conditioning on the Initial State

Raghavan and Baum's ROVA applies only to codes that begin and end at a known state. Each of the probabilities $f(y|x')$ in (2) is implicitly conditioned on the event that the receiver knows the initial and final state of the convolutional encoder.

To be precise, ROVA beginning and ending at the same state s , which we shall denote as $\text{ROVA}(s)$, effectively computes the following:

$$\underbrace{P(\hat{x}_s|y, s)}_{\text{computed by ROVA}(s)} = \frac{f(y|\hat{x}_s, s)P(\hat{x}_s|s)}{f(y|s)} = \frac{f(y|\hat{x}_s, s)}{\sum_{x'_s} f(y|x'_s, s)}, \quad (3)$$

where x'_s denotes that the sum is over all codewords x' with starting state s , and $f(y|x'_s, s)$ is shorthand for $f(Y = y|X = x'_s, S = s)$. In summary, $\text{ROVA}(s)$ computes the ML codeword \hat{x}_s corresponding to starting state s , the posterior probability of that codeword given s , $P(\hat{x}_s|y, s)$, and the probability of the received sequence given s , $f(y|s)$. The inputs and outputs of $\text{ROVA}(s)$ are illustrated in the block diagram of Fig. 1.

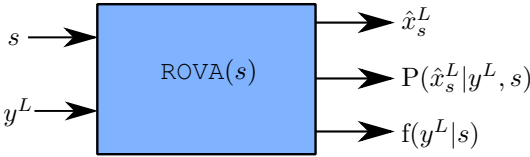


Fig. 1. Block diagram of Raghavan and Baum's $\text{ROVA}(s)$ [1].

For tail-biting codes, we are interested in computing the quantity $P(\hat{x}|y)$ without conditioning on the unknown starting and ending state s :

$$P(\hat{x}|y) = \sum_s P(\hat{x}|y, s)P(s|y). \quad (4)$$

Throughout this paper, we assume that a feedforward convolutional encoder is used, so that the n -tuple of coded symbols x_ℓ in trellis segment ℓ depends only on the most recent $\nu + 1$ input-symbol k -tuples. The ML codeword \hat{x} has an associated initial state, \hat{s} . Moreover, $P(\hat{x}|y, s) = 0$ unless $s = \hat{s}$, since \hat{x} is not a possible codeword for any starting state other than \hat{s} . Thus, we have:

$$P(\hat{x}|y) = P(\hat{x}|y, \hat{s})P(\hat{s}|y). \quad (5)$$

Thus, the tail-biting ROVA (TB ROVA) must compute the probability $P(\hat{x}|y)$ of successful decoding in (5) by weighting $P(\hat{x}|y, \hat{s})$ with $P(\hat{s}|y)$. (For the original ROVA with a known starting state \hat{s} , $P(\hat{s}|y) = 1$ and $P(s'|y) = 0 \forall s' \neq \hat{s}$.)

Using the fact that each of the initial states s is equally likely *a priori* (i.e., $P(s) = P(s') \forall s \neq s'$), we have:

$$P(\hat{s}|y) = \frac{f(y|\hat{s})}{\sum_{s'} f(y|s')}. \quad (6)$$

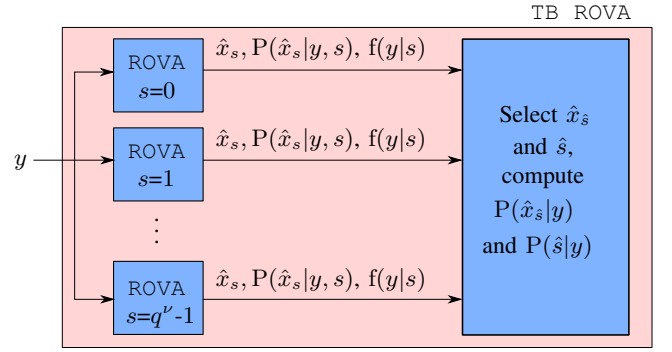


Fig. 2. Block diagram of the straightforward tail-biting ROVA (TB ROVA).

This finally yields

$$\underbrace{P(\hat{x}|y)}_{\text{computed by TB ROVA}} = \frac{\overbrace{P(\hat{x}|y, \hat{s})f(y|\hat{s})}^{\text{computed by ROVA}(\hat{s})}}{\sum_{s'} \underbrace{f(y|s')}_{\text{computed by ROVA}(s')}}}, \quad (7)$$

where the summation in the denominator of (7) is over all q^ν possible initial states.

B. A Straightforward Tail-biting ROVA

A straightforward ML approach to decoding tail-biting codes is to perform the Viterbi algorithm $\text{VA}(s)$, for each possible starting state $s = 0, 1, \dots, q^\nu - 1$. The ML codeword \hat{x} is then chosen by determining the starting state with the greatest path metric (i.e., the greatest probability). As shown in Fig. 2, this approach will work for the ROVA as well: perform $\text{ROVA}(s)$ for each possible s and then pick \hat{x} and its starting state \hat{s} . The probability $P(\hat{x}|y)$ is then computed as in (7), using $P(\hat{x}|y, \hat{s})$ from the ROVA for the ML starting state and the $f(y|s)$ terms produced by the ROVAs for all the states. This approach is illustrated in the block diagram of Fig. 2.

III. POST-DECODING RELIABILITY COMPUTATION

There are q^ν possible starting states that must be evaluated in the straightforward approach of Fig. 2. Thus it may be beneficial to instead use an existing reduced-complexity tail-biting decoder to find \hat{x} , and then compute the reliability separately. Many reduced-complexity tail-biting decoders take advantage of the circular decoding property of tail-biting codes. Some of these approaches are not maximum likelihood, such as the wrap-around Viterbi algorithm or Bidirectional Viterbi Algorithm (BVA), both discussed in [21]. The A* algorithm [23]–[25] is one ML alternative to the tail-biting decoding method described in Sec. II-B. Its complexity depends on the SNR.

Suppose that a decoder has already been used to determine \hat{x} and its starting state \hat{s} , and that we would like to determine $P(\hat{x}|y)$. One operation of $\text{ROVA}(\hat{s})$ would compute the probability $P(\hat{x}|y, \hat{s})$, but the probability $P(\hat{s}|y)$ required by (5) would still be undetermined. Must we perform $\text{ROVA}(s)$ for each $s \neq \hat{s}$ in order to compute $P(\hat{s}|y)$ as in (6)? This section shows how to avoid this by combining the computations

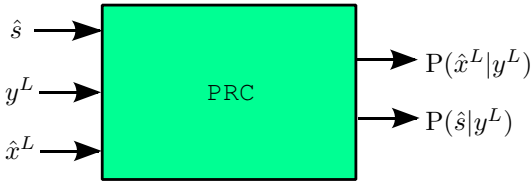


Fig. 3. Block diagram of the Post-decoding Reliability Computation (PRC).

of the straightforward approach into a novel Post-decoding Reliability Computation (PRC) for tail-biting codes.

Fig. 3 shows a block diagram of PRC. For a rate- k/n tail-biting convolutional code with ν memory elements, PRC takes the following inputs: a received sequence y^L with $L = N/n$ trellis segments, a *candidate codeword* \hat{x}^L corresponding to a *candidate path* in the trellis, and the starting/ending state \hat{s} of the candidate codeword. The goal is to compute the posterior probability of the candidate codeword, $P(\hat{x}^L|y^L)$. The candidate codeword selected by the decoder may not be the ML codeword. PRC computes its true reliability regardless.

Raghavan and Baum's ROVA [1] performs the traditional add-compare-select operations of the Viterbi algorithm and then computes, for every state in each trellis segment, the posterior probability that the survivor path is correct and the posterior probability that one of the non-surviving paths at the state is correct. Upon reaching the end of the trellis (the L th segment), having selected survivor paths at each state, there will be one survivor path corresponding to the ML codeword.

In contrast, with the candidate path already identified, PRC processes the trellis without explicitly selecting survivors. PRC computes the reliability of the candidate path and the overall reliability of all other paths.

A. PRC Overview

We define the following events at trellis stage ℓ ($\ell \in \{1, 2, \dots, L\}$):

- $p_j^\ell = \{\text{the candidate path from its beginning at state } \hat{s} \text{ to its arrival at state } j \text{ in segment } \ell \text{ is correct}\}$
- $\bar{p}_r^\ell(s) = \{\text{some path from its beginning at state } s \text{ to its arrival at state } r \text{ in segment } \ell \text{ is correct (including possibly the candidate path if } \hat{s} = s)\}$
- $b_{ij}^\ell = \{\text{the branch from state } i \text{ to state } j \text{ at time } \ell \text{ is correct}\}$

For $\nu = 3$ memory elements, Fig. 4 gives some examples of the paths corresponding to each of these events. The black branches in Fig. 4 constitute all of the paths in the event $\bar{p}_r^\ell(s)$. The red branches in Fig. 4 show the candidate path corresponding to the event p_j^ℓ . The posterior probability that the red candidate path starting at state \hat{s} is correct is $P(p_j^\ell|y^\ell)$. The posterior probability that any of the paths that started at state s and arrive at state r in segment 7 are correct is $P(\bar{p}_r^7(s)|y^7)$. Note that since some branch transitions are invalid in the trellis, $P(p_j^\ell)$ and $P(b_{ij}^\ell)$ may be zero for invalid states and branches in segment ℓ .

The path-correct probabilities $P(p_j^\ell)$ and $P(\bar{p}_r^\ell(s))$ can be expressed recursively in terms of the probabilities of the previous trellis segments' paths being correct. Conditioned on

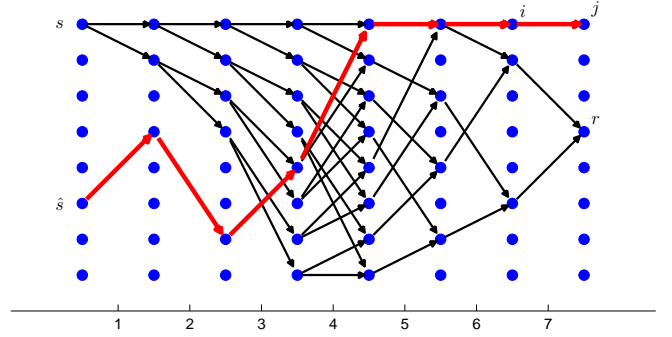


Fig. 4. An example of a trellis for a rate- $1/n$ code with $\nu = 3$ memory elements is shown for $\ell = 1, 2, \dots, 7$. The red branches show the candidate path from its beginning at state \hat{s} to its arrival at state j . The black branches show all of the paths originating at state s from their beginning to their arrival at state r . Note that the figure does not show the final stage of the tail-biting trellis where all paths must return to their starting states.

the noisy channel observations $y^\ell = (y_1, y_2, \dots, y_\ell)$, the path-correct probability for the candidate path is

$$P(p_j^\ell|y^\ell) = P(p_i^{\ell-1}, b_{ij}^\ell|y^\ell) \quad (8)$$

$$= P(b_{ij}^\ell|y^\ell, p_i^{\ell-1})P(p_i^{\ell-1}|y^\ell) \quad (9)$$

$$= \frac{f(y_\ell|y^{\ell-1}, p_i^{\ell-1}, b_{ij}^\ell)}{f(y_\ell|y^{\ell-1})} \quad (10)$$

$$\times P(b_{ij}^\ell|y^{\ell-1}, p_i^{\ell-1})P(p_i^{\ell-1}|y^{\ell-1}).$$

The decomposition in (10) uses Bayes' rule and follows [1]. Fig. 4 identifies an example of states i and j used to compute the probability of b_{ij}^ℓ .

By the Markov property, $f(y_\ell|y^{\ell-1}, p_i^{\ell-1}, b_{ij}^\ell) = f(y_\ell|b_{ij}^\ell)$, which is the conditional p.d.f., related to the familiar Viterbi algorithm branch metric. Similarly, the second term is $P(b_{ij}^\ell|y^{\ell-1}, p_i^{\ell-1}) = P(b_{ij}^\ell|p_i^{\ell-1})$. With these simplifications, (10) becomes

$$P(p_j^\ell|y^\ell) = \frac{f(y_\ell|b_{ij}^\ell)P(b_{ij}^\ell|p_i^{\ell-1})P(p_i^{\ell-1}|y^{\ell-1})}{f(y_\ell|y^{\ell-1})}. \quad (11)$$

The denominator can be expressed as a sum over all branches in the trellis \mathcal{T}_ℓ at time ℓ , where each branch from m to r is denoted by a pair $(m, r) \in \mathcal{T}_\ell$:

$$f(y_\ell|y^{\ell-1}) = \sum_{(m,r) \in \mathcal{T}_\ell} f(y_\ell|y^{\ell-1}, b_{mr}^\ell)P(b_{mr}^\ell|y^{\ell-1}) \quad (12)$$

$$= \sum_{(m,r) \in \mathcal{T}_\ell} f(y_\ell|b_{mr}^\ell)P(b_{mr}^\ell|y^{\ell-1}). \quad (13)$$

The derivation thus far has followed [1], which focused on terminated convolutional codes.

For tail-biting codes, we can further expand the term $P(b_{mr}^\ell|y^{\ell-1})$ by summing over all the possible starting states s' as follows:

$$P(b_{mr}^\ell|y^{\ell-1}) = \sum_{s'} P(b_{mr}^\ell, \bar{p}_m^{\ell-1}(s')|y^{\ell-1}) \quad (14)$$

$$= \sum_{s'} P(b_{mr}^\ell|y^{\ell-1}, \bar{p}_m^{\ell-1}(s'))P(\bar{p}_m^{\ell-1}(s')|y^{\ell-1})$$

$$= \sum_{s'} P(b_{mr}^\ell|\bar{p}_m^{\ell-1}(s'))P(\bar{p}_m^{\ell-1}(s')|y^{\ell-1}), \quad (15)$$

where the last equality follows from the Markov property $P(b_{mr}^\ell | y^{\ell-1}, \bar{p}_m^{\ell-1}(s')) = P(b_{mr}^\ell | \bar{p}_m^{\ell-1}(s'))$. Thus, (13) becomes

$$f(y_\ell | y^{\ell-1}) = \sum_{(m,r) \in \mathcal{T}_\ell} f(y_\ell | b_{mr}^\ell) \times \sum_{s'} P(b_{mr}^\ell | \bar{p}_m^{\ell-1}(s')) P(\bar{p}_m^{\ell-1}(s') | y^{\ell-1}). \quad (16)$$

The term $P(b_{mr}^\ell | \bar{p}_m^{\ell-1}(s'))$ is the probability that the branch from state m to state r is correct, given that one of the paths that started at state s' and arrived at state m at time $\ell - 1$ is correct. Define $K = L - \nu$. $P(b_{mr}^\ell | \bar{p}_m^{\ell-1}(s')) = q^{-k}$ for $1 \leq \ell \leq K$ (i.e., all ℓ except for the last ν trellis segments). This is because there are q^k equiprobable next states for these values of ℓ .

Using the notation $r \rightarrow s'$ to indicate there is a valid path from state r at time ℓ to state s' at time L , we define the following indicator function $I(b_{mr}^\ell, s')$, which indicates that the trellis branch from state m to state r at trellis stage ℓ is a branch in a possible trellis path that terminates at s' :

$$I(b_{mr}^\ell, s') = \begin{cases} 1, & 1 \leq \ell \leq K, & (m, r) \in \mathcal{T}_\ell, \\ 1, & K + 1 \leq \ell \leq L, & (m, r) \in \mathcal{T}_\ell, \quad r \rightarrow s' \\ 0, & K + 1 \leq \ell \leq L, & (m, r) \in \mathcal{T}_\ell, \quad r \not\rightarrow s' \\ 0, & & (m, r) \notin \mathcal{T}_\ell, \end{cases} \quad (17)$$

The branch-correct probabilities can now be written as

$$P(b_{mr}^\ell | \bar{p}_m^{\ell-1}(s')) = \begin{cases} I(b_{mr}^\ell, s') q^{-k}, & 1 \leq \ell \leq K \\ I(b_{mr}^\ell, s'), & K + 1 \leq \ell \leq L \end{cases} \quad (18)$$

$$P(b_{mr}^\ell | \bar{p}_m^{\ell-1}) = \begin{cases} I(b_{mr}^\ell, \hat{s}) q^{-k}, & 1 \leq \ell \leq K \\ I(b_{mr}^\ell, \hat{s}), & K + 1 \leq \ell \leq L. \end{cases} \quad (19)$$

We now define the following normalization term for the ℓ th trellis segment using the above indicators:

$$\Delta_\ell = \sum_{(m,r) \in \mathcal{T}_\ell} f(y_\ell | b_{mr}^\ell) \sum_{s'} I(b_{mr}^\ell, s') P(\bar{p}_m^{\ell-1}(s') | y^{\ell-1}) \quad (20)$$

$$= \begin{cases} f(y_\ell | y^{\ell-1}) q^k, & 1 \leq \ell \leq K \\ f(y_\ell | y^{\ell-1}), & K + 1 \leq \ell \leq L. \end{cases} \quad (21)$$

The Δ_ℓ normalization term includes most of (16) but excludes $P(b_{mr}^\ell | \bar{p}_m^{\ell-1}(s'))$ because it cancels with $P(b_{ij}^\ell | \bar{p}_i^{\ell-1})$ in the numerator of (11). (Either both are q^{-k} or both are 1, depending only on ℓ .) Substituting (21) into (11), we have

$$P(p_j^\ell | y^\ell) = \frac{1}{\Delta_\ell} f(y_\ell | b_{ij}^\ell) P(\bar{p}_i^{\ell-1} | y^{\ell-1}). \quad (22)$$

Thus, for the ℓ th trellis segment, (22) expresses the candidate path-correct probability in terms of the candidate path-correct probability in the previous segment. Note that in the middle portion of the trellis ($\nu + 1 \leq \ell \leq K$), $\Delta_\ell = \sum_{(m,n) \in \mathcal{T}_\ell} f(y_\ell | b_{mr}^\ell) P(\bar{p}_m^{\ell-1} | y^{\ell-1})$, where

$P(\bar{p}_m^{\ell-1} | y^{\ell-1}) = \sum_{s'} P(\bar{p}_m^{\ell-1}(s') | y^{\ell-1})$, the sum of all path probabilities from all the starting states.

The corresponding expression for the overall path probabilities $P(\bar{p}_r^\ell(s) | y^\ell)$ involves more terms. Instead of tracing a single candidate path through the trellis, we must add the probabilities of all the valid tail-biting paths incident on state r in segment ℓ as follows:

$$P(\bar{p}_r^\ell(s) | y^\ell) = \sum_{m: (m,r) \in \mathcal{T}_\ell} \frac{f(y_\ell | b_{mr}^\ell) I(b_{mr}^\ell, s) P(\bar{p}_m^{\ell-1}(s) | y^{\ell-1})}{\Delta_\ell}. \quad (23)$$

The summation above is over the q^k incoming branches to state r . In the special case of a rate- $\frac{1}{n}$ binary code ($q=2$), there are 2 incoming branches, which we will label as (m, r) and (u, r) , so (23) becomes

$$P(\bar{p}_r^\ell(s) | y^\ell) = \frac{1}{\Delta_\ell} [f(y_\ell | b_{mr}^\ell) I(b_{mr}^\ell, s) P(\bar{p}_m^{\ell-1}(s) | y^{\ell-1}) + f(y_\ell | b_{ur}^\ell) I(b_{ur}^\ell, s) P(\bar{p}_u^{\ell-1}(s) | y^{\ell-1})]. \quad (24)$$

Fig. 4 illustrates how the paths from starting state s merge into state r at trellis segment $\ell = 7$.

B. PRC Algorithm Summary

The path probabilities are initialized as follows:

- $P(p_j^0 | y^0) = P(\hat{s}) = q^{-\nu}$ if $\hat{s} = j$, or 0 otherwise.
- $P(\bar{p}_r^0(s) | y^0) = P(s) = q^{-\nu}$ if $s = r$, or 0 otherwise.

In each trellis-segment ℓ ($1 \leq \ell \leq L$), do the following:

- 1) For each branch $(m, r) \in \mathcal{T}_\ell$, compute the conditional p.d.f. $f(y_\ell | b_{mr}^\ell)$.
- 2) For each branch $(m, r) \in \mathcal{T}_\ell$ and each starting state s , compute the branch-valid indicator $I(b_{mr}^\ell, s)$, as in (17).
- 3) Using the above values, compute the normalization constant Δ_ℓ , as in (20).
- 4) For the current state j of the candidate path, compute the candidate path-correct probability $P(p_j^\ell | y^\ell)$, as in (22).
- 5) For each starting state s and each state r , compute the overall path-correct probabilities $P(\bar{p}_r^\ell(s) | y^\ell)$, as in (23).

After processing all L stages of the trellis, the following meaningful quantities emerge:

- The posterior probability that the tail-biting candidate path from \hat{s} to \hat{s} is correct is $P(p_{\hat{s}}^L | y^L) = P(\hat{x}^L | y^L)$, which is the probability that the decoded word is correct, given the received sequence.
- The posterior word-error probability is then $1 - P(p_{\hat{s}}^L | y^L) = 1 - P(\hat{x}^L | y^L)$.
- The posterior probability that any of the tail-biting paths (any of the codewords) from s to s is correct is $P(\bar{p}_s^L(s) | y^L) = P(s | y^L)$, which is the state reliability desired for (5).

Numerical results of PRC are shown in Fig. 7 in Sec. VIII.

IV. THE TAIL-BITING STATE-ESTIMATION ALGORITHM

The Post-decoding Reliability Computation described above relies on a separate decoder to identify the candidate path. If, on the other hand, we would like to compute the word-error

probability of a tail-biting code without first having determined a candidate path and starting state, we may use the following Tail-Biting State-Estimation Algorithm (TB SEA). TB SEA computes the MAP starting state $\hat{s} = \arg \max_{s'} P(s'|y^L)$, along with its reliability $P(\hat{s}|y^L)$. ROVA(\hat{s}) can then be used to determine the MAP codeword $\hat{x}_{\hat{s}}$ corresponding to starting state \hat{s} , as illustrated in Fig. 5.

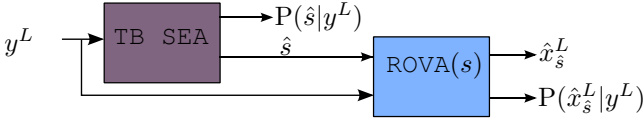


Fig. 5. Block diagram of the Tail-Biting State-Estimation Algorithm (TB SEA), followed by ROVA(\hat{s}) for the ML starting state \hat{s} .

PRC relied on tracing a single candidate path through the trellis and computing the candidate path-correct probability, as in (22). However, the overall path-correct probabilities in (23) do not rely on the candidate path or its probability. The proposed TB SEA aggregates all the previous-segment path-correct probabilities $P(\bar{p}_m^{\ell-1}(s)|y^{\ell-1})$ as in (23), without regard to a candidate path. As a result, TB SEA replaces the traditional add-compare-select operations of the Viterbi algorithm with the addition of all the path probabilities merging into a state that emanate from a particular origin state. Once the entire trellis has been processed, the state reliabilities are compared and the MAP starting state is selected.

A. TB SEA Algorithm Summary

The path probabilities are initialized as follows:

- $P(\bar{p}_r^0(s)|y^0) = P(s) = q^{-\nu}$ if $s = r$, or 0 otherwise.

In each trellis-segment ℓ ($1 \leq \ell \leq L$), do the following:

- 1) For each branch $(m, r) \in \mathcal{T}_\ell$, compute the conditional p.d.f. $f(y_\ell|b_{mr}^\ell)$.
- 2) For each branch $(m, r) \in \mathcal{T}_\ell$ and each starting state s , compute the branch-valid indicator $I(b_{mr}^\ell, s)$, as in (17).
- 3) Using the above values, compute the normalization constant Δ_ℓ , as in (20).
- 4) For each starting state s and each state r , compute the overall path-correct probabilities $P(\bar{p}_r^\ell(s)|y^\ell)$, as in (23).

After processing all L stages of the trellis, the following meaningful quantity emerges:

- The posterior probability that any of the tail-biting paths (any of the codewords) from s to s is correct is $P(\bar{p}_s^L(s)|y^L) = P(s|y^L)$.

TB SEA selects the starting state with the maximum value of $P(s|y^L)$ (the MAP choice of starting state), yielding \hat{s} and its reliability $P(\hat{s}|y^L)$. Thus, TB SEA has selected the MAP starting state without explicitly evaluating all possible codewords (i.e., paths through the trellis). This can be applied to other applications besides coding to efficiently compute the MAP starting state of a tail-biting, finite-state Markov process.

B. TB SEA + ROVA(\hat{s})

After finding the MAP starting state \hat{s} with TB SEA, ROVA(\hat{s}) may be used to compute the MAP codeword $\hat{x}_{\hat{s}}^L$

and $P(\hat{x}_{\hat{s}}^L|y^L, \hat{s})$. We have used the subscript \hat{s} to indicate that $\hat{x}_{\hat{s}}^L$ is the MAP codeword for the terminated code starting and ending in \hat{s} . The overall reliability $P(\hat{x}_{\hat{s}}^L|y^L)$ can then be computed as in (5), which we have replicated below to show how the TB SEA and ROVA(\hat{s}) provide the needed factors:

$$P(\hat{x}|y) = \underbrace{P(\hat{x}|y, \hat{s})}_{\text{computed by ROVA}(\hat{s})} \times \underbrace{P(\hat{s}|y)}_{\text{computed by TB SEA}} \quad (25)$$

C. MAP States vs. MAP Codewords

Is it possible that the maximum a posteriori codeword \hat{x} corresponds to a starting state other than the MAP state \hat{s} ? The following theorem proves that the answer is no, given a suitable probability of error.

Theorem 1. *The MAP codeword \hat{x} for a tail-biting convolutional code begins and ends in the MAP state \hat{s} , as long as $P(\hat{x}|y) > \frac{1}{2}$.*

Proof: Consider a codeword \hat{x} with $P(\hat{x}|y) > \frac{1}{2}$. By (5), $P(\hat{x}|y) = P(\hat{x}|y, s_{\hat{x}})P(s_{\hat{x}}|y)$, where $s_{\hat{x}}$ is the starting state of \hat{x} . This implies that $P(s_{\hat{x}}|y) > \frac{1}{2}$. The MAP state is $\arg \max_{s'} P(s'|y)$, which must be $s_{\hat{x}}$, since all other states s' must have $P(s'|y) < \frac{1}{2}$. ■

Theorem 1 shows that the application of TB SEA followed by the Viterbi algorithm (or the ROVA) will always yield the MAP codeword \hat{x} of the tail-biting code, not just the MAP codeword for the terminated code starting in \hat{s} (as long as the probability of error is less than 1/2). In most practical scenarios, the word-error probability $(1 - P(\hat{x}|y))$, even if unknown exactly, is much less than $\frac{1}{2}$, so the theorem holds. As a result, in these cases TB SEA selects the same codeword \hat{x} as would the TB ROVA of Sec. II-B, and computes the same reliability $P(\hat{x}|y)$.

V. THE SIMPLIFIED ROVA FOR TAIL-BITING CODES

This section proposes replacing the exact word-error computations of Sec. II-B's straightforward TB ROVA with an estimated word-error probability, using Fricke and Hoehner's simplified (approximate) ROVA [4]. In contrast to TB SEA, this approach requires a Viterbi decoder for each starting state to select the ML codeword for that state. Fricke and Hoehner's [4] simplified ROVA for starting state s , which we call *Approx ROVA*(s), estimates the probability $P(x_s|y, s)$. Substituting this estimate $\tilde{P}(x_s|y, s)$ into (7), we have the following approximation:

$$\tilde{P}(\hat{x}|y) = \frac{\overbrace{\tilde{P}(\hat{x}|y, \hat{s})}^{\text{computed by Approx ROVA}(\hat{s})} f(y|\hat{s})}{\sum_s f(y|s)}. \quad (26)$$

While $f(y|s)$ is not computed directly by *Approx ROVA*(s), we can approximate it with quantities available from *Approx*

ROVA(s) as

$$\tilde{f}(y|s) \approx \tilde{f}(y|s) = \frac{f(y|x_s, s)P(x_s|s)}{\tilde{P}(x_s|y, s)} \quad (27)$$

$$= \frac{f(y|x_s, s)}{q^K \tilde{P}(x_s|y, s)}, \quad (28)$$

when all q^K codewords with starting state s are equally likely. Note $f(y|x_s, s)$ can be calculated by the Viterbi algorithm for starting state s .

Equations (26) and (28) lead to the following estimate of the word-correct probability:

$$\tilde{P}(\hat{x}|y) = \frac{\substack{\text{computed by Approx ROVA}(\hat{s}) \\ \tilde{P}(\hat{x}|y, \hat{s})\tilde{f}(y|\hat{s})}}{\sum_s \substack{\text{computed by Approx ROVA}(s) \\ \tilde{f}(y|s)}}. \quad (29)$$

We refer to the overall computation of $\tilde{P}(\hat{x}|y)$ as `Approx TB ROVA`. Sec. VII provides a discussion of complexity, and Sec. VIII presents simulation results.

Note that despite the approximations, the simplified ROVA chooses the ML codeword for terminated codes. For the tail-biting version `Approx TB ROVA`, as long as the winning path metric of each starting/ending state is used to determine the ML state \hat{s} , the decoded codeword will also be ML (and the same as the codeword chosen by the exact tail-biting ROVA in Sec. II-B). However, if the approximate reliabilities $\tilde{P}(x_s|y, s)$ are used instead of the path metrics to select the decoded word \hat{x} as $\hat{x} = \arg \max_s \tilde{P}(x_s|y, s)$, it is possible that the decoded word will not be ML (if the channel is noisy enough).

VI. THE TB BCJR ALGORITHM FOR STATE ESTIMATION

While several related papers such as [17] and [18] have proposed ways to estimate the starting state of a tail-biting decoder, none computes exactly the posterior probability of the starting state, $P(s|y^L)$, as described for TB SEA in Sec. IV. Upon a first inspection, the tail-biting BCJR (TB BCJR) of [12] appears to provide a similar method of computing this probability. Applying the forward recursion of the BCJR algorithm provides posterior probabilities that are denoted as

$\alpha_L(s) = P(s|y^L)$ in [12]. Thus, it would appear that the state-estimation algorithm of Sec. IV can be replaced by a portion of the TB BCJR algorithm. This would yield a significant decrease in computational complexity, from roughly $q^{2\nu}$ operations per trellis segment for TB SEA to q^ν for the TB BCJR. However, as will be shown in Sec. VIII, the word-error performance of the tail-biting BCJR when used in this manner is significantly inferior to that of TB SEA.

As noted in [14] and [15], the tail-biting BCJR algorithm is an approximate symbol-by-symbol MAP decoder. It is approximate in the sense that the forward recursion of the TB BCJR in [12] does not strictly enforce the tail-biting restriction, allowing non-tail-biting ‘‘pseudocodewords’’ to appear and cause errors. [12] requires the probability distributions of the starting and ending states to be the same, which is a weaker condition than requiring all codewords to start and end in the same state. [14] and [15] have shown that when the tail-biting length L is large relative to the memory length ν , the suboptimality of the TB BCJR in terms of the bit-error rate is small. However, we are concerned with word-error performance in this paper. We find that when the TB BCJR is used to estimate the initial state \hat{s} and its probability $P(\hat{s}|y^L)$, followed by the `ROVA`(\hat{s}) for the most likely state \hat{s} , the impact on word error is severe (Fig. 8). Frequent state-estimation errors prevent the Viterbi algorithm in the second phase from decoding to the correct codeword. Thus, the approximate tail-biting BCJR of [12] is not effective as a replacement for TB SEA when using the word-error criterion.

In contrast, the exact symbol-by-symbol MAP decoder for tail-biting codes in [16, Ch. 7] does enforce the tail-biting restriction, and has complexity on the same order as that of TB SEA. However, because the symbol-by-symbol MAP decoder selects the most probable input symbols while TB SEA + `ROVA`(\hat{s}) selects the most probable input sequence, TB SEA + `ROVA`(\hat{s}) is recommended for use in retransmission schemes that depend on the word-error probability.

VII. COMPLEXITY ANALYSIS

Table I compares the complexity per trellis segment of each of the discussed algorithms, assuming that the conditional p.d.f. $f(y_\ell|b_{m_r}^\ell)$ has already been computed for every branch in

TABLE I
COMPLEXITY PER TRELLIS SEGMENT OF THE PROPOSED ALGORITHMS (DISREGARDING BRANCH METRIC COMPUTATIONS).

Algorithm	Path metrics	Cand. prob.	Overall prob.	Additions	Multiplications	Divisions
Key modules of decoders						
VA(s)	q^ν	0	0	0	$q^{\nu+k}$	0
ROVA(s) [1]	q^ν	q^ν	q^ν	$2q^\nu(2q^k - 1) - 1$	$3q^{\nu+k}$	$2q^\nu$
PRC	0	1	$q^{2\nu}$	$q^{2\nu}(2q^k - 1) - 1$	$q^{2\nu+k}$	$q^{2\nu} + 1$
TB SEA	0	0	$q^{2\nu}$	$q^{2\nu}(2q^k - 1) - 1$	$q^{2\nu+k}$	$q^{2\nu}$
Approx ROVA(s) [4]	q^ν	q^ν	0	$q^\nu(q^k - 1)$	$q^{\nu+k} + 1$	q^ν
Tail-biting decoders that provide reliability output						
TB ROVA	$q^{2\nu}$	$q^{2\nu}$	$q^{2\nu}$	$2q^{2\nu}(2q^k - 1) - q^\nu$	$3q^{2\nu+k}$	$2q^{2\nu}$
TB SEA + ROVA(\hat{s})	q^ν	q^ν	$q^{2\nu} + q^\nu$	$(q^{2\nu} + 2q^\nu)(2q^k - 1) - 2$	$q^{2\nu+k} + 3q^{\nu+k}$	$q^{2\nu} + 2q^\nu$
Approx TB ROVA	$q^{2\nu}$	$q^{2\nu}$	0	$q^{2\nu}(q^k - 1)$	$q^{2\nu+k} + q^\nu$	$q^{2\nu}$

the trellis. The columns labeled ‘Path metrics’, ‘Cand. prob.’, and ‘Overall prob.’ refer to the number of quantities that must be computed and stored in every trellis segment, for the path metrics of the Viterbi algorithm, the candidate path probability of (22), and the overall path probability of (23), respectively. The number of operations per trellis segment required to compute these values is listed in the columns labeled ‘Additions’, ‘Multiplications’, and ‘Divisions’.

The ROVA (s) row of Table I corresponds to Raghavan and Baum’s ROVA [1] for a terminated code starting and ending in state s . The operations listed include the multiplications required for the path metric computations of the Viterbi algorithm for state s , $VA(s)$. The TB ROVA row represents performing the ROVA for each of the q^ν possible starting states as described in Sec. II-B, so each of the quantities is multiplied by q^ν .

The PRC row corresponds to the proposed Post-Decoding Reliability Computation of Sec. III. The complexity incurred to determine the candidate path (e.g., by the BVA or the A* algorithm) is not included in this row and must also be accounted for, which is why no path metrics are listed for PRC. Compared to TB ROVA, due to combining computations into a single pass through the trellis the complexity of PRC is reduced by approximately a factor of 2. This is because TB ROVA calculates a candidate path probability for each of the q^ν starting states (due to decoding to the ML codeword each time), whereas the combined trellis-processing of PRC involves only one candidate path. Both algorithms compute q^ν overall path probabilities, so the ratio of complexity is roughly $\frac{1+q^\nu}{q^\nu+q^\nu} \approx \frac{1}{2}$.

The reduction in complexity of TB SEA compared to PRC is modest, with slightly fewer multiplications and divisions required due to the absence of the candidate path calculations in TB SEA. Importantly, performing TB SEA followed by ROVA(\hat{s}) for the ML state \hat{s} is shown to be an improvement over TB ROVA for moderately large ν . TB SEA + ROVA(\hat{s}) requires approximately one half the additions, one third the multiplications, and one half the divisions of TB ROVA. TB SEA’s complexity reduction is partly due to the fact that it does not require the add-compare-select operations of the Viterbi algorithm, which TB ROVA performs for each starting state. Note also that the number of trellis segments processed in TB SEA is constant (L segments), whereas the number of trellis segments processed by many tail-biting decoders (e.g., the BVA) depends on the SNR.

Lastly, the computational costs of performing Fricke and Hoehner’s simplified ROVA [4] are listed in the Approx ROVA(s) row, along with the tail-biting approximate version of Sec. V (Approx TB ROVA). In both of these cases, the word-error outputs are estimates. In contrast, TB ROVA and TB SEA + ROVA(\hat{s}) compute the exact word-error probability of the received word.

For the special case of rate-1/ n binary convolutional codes with $\nu = 6$ memory elements, Fig. 6 gives an example of the number of additions, multiplications, and divisions that must be performed per trellis segment for the three tail-biting decoders in Table I. TB SEA + ROVA(\hat{s}) is competitive with Approx TB ROVA in terms of the number of multiplications

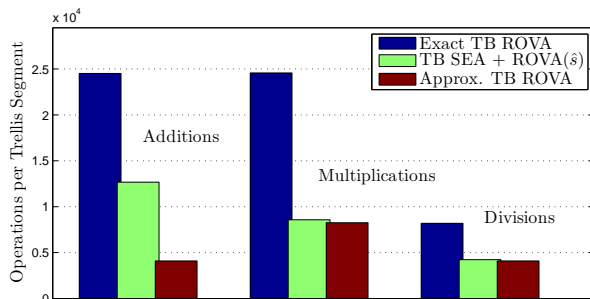


Fig. 6. Examples of the computations per trellis segment for the tail-biting decoders listed in Table I corresponding to rate-1/ n binary convolutional codes, for $\nu = 6$ memory elements.

TABLE II

GENERATOR POLYNOMIALS g_1, g_2 , AND g_3 CORRESPONDING TO THE SIMULATED RATE-1/3 TAIL-BITING CONVOLUTIONAL CODE. d_{free} IS THE FREE DISTANCE, $A_{d_{free}}$ IS THE NUMBER OF NEAREST NEIGHBORS WITH WEIGHT d_{free} , AND L_D IS THE ANALYTIC TRACEBACK DEPTH.

ν	2^ν	g_1	g_2	g_3	d_{free}	$A_{d_{free}}$	L_D
6	64	117	127	155	15	3	21

and divisions that must be performed. Our software simulations have shown that the speedup of TB SEA + ROVA(\hat{s}) compared to TB ROVA and even to Approx TB ROVA is more drastic than Table I and Fig. 6 suggest, due to the many for loops for each starting state that are used in TB ROVA and Approx TB ROVA.

VIII. NUMERICAL RESULTS

A. Convolutional Codes

Table II lists the rate-1/3, binary convolutional encoder polynomials from Lin and Costello [3, Table 12.1] used in the simulations. The number of memory elements is ν , 2^ν is the number of states, and $\{g_1, g_2, g_3\}$ are the generator polynomials in octal notation. The code selected has the optimum free distance d_{free} , which is listed along with the analytic traceback depth L_D [26]. $A_{d_{free}}$ is the number of nearest neighbors with weight d_{free} .

B. Additive White Gaussian Noise (AWGN) Channel

For antipodal signaling (i.e., BPSK) over the Gaussian channel, the conditional density $f(y_\ell | b_{ij}^\ell)$ can be expressed as

$$f(y_\ell | b_{ij}^\ell) = \prod_{m=1}^n \frac{1}{\sqrt{2\pi\sigma^2}} \exp \left\{ -\frac{[y_\ell(m) - x_\ell(m)]^2}{2\sigma^2} \right\}, \quad (30)$$

where $y_\ell(m)$ is the m th received symbol in trellis-segment ℓ , $x_\ell(m)$ is the m th output symbol of the encoder branch from state i to state j in trellis segment ℓ , and σ^2 is the noise variance. For a transmitter power constraint P , the encoder output symbols are $x_\ell(m) \in \{+\sqrt{P}, -\sqrt{P}\}$ and the energy per bit is $E_b = P \frac{n}{k}$. This yields an SNR equal to $P/\sigma^2 = 2 \frac{k}{n} \frac{E_b}{N_0}$ when the noise variance is $\sigma^2 = N_0/2$.

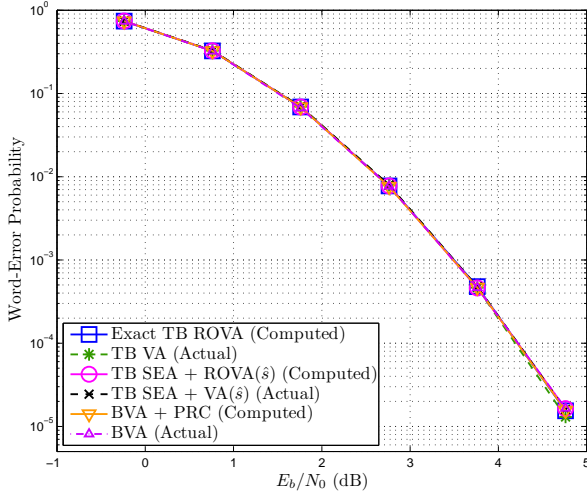


Fig. 7. Computed and actual word-error probability of the exact TB ROVA, TB SEA followed by ROVA(\hat{s}), and the Bidirectional Viterbi Algorithm (BVA) followed by the Post-decoding Reliability Computation (PRC), on the AWGN channel. All simulations use the rate-1/3, 64-state convolutional code listed in Table II with $L = 128$ input bits and 384 output bits. The ‘Computed’ values are the word-error probabilities calculated by the receiver (averaged over the simulation) and the ‘Actual’ values count the number of words decoded incorrectly.

C. Simulation Results

This section provides a comparison of the average word-error probability computed by the tail-biting reliability-output algorithms for the AWGN channel and the rate-1/3, 64-state tail-biting convolutional code listed in Table II. Fig. 7 and Fig. 8 use $L = 128$ input bits and 384 output bits. The ‘Actual’ curves in the figures show the fraction of codewords that are decoded incorrectly, whereas the ‘Computed’ curves show the word-error probability computed by the receiver. For both Fig. 7 and Fig. 8, ‘Actual’ values are only plotted for simulations with more than 100 codewords in error.

Fig. 7 evaluates the performance of Sec. II-B’s TB ROVA and Sec. III’s PRC. In the figure, PRC is applied to the output of the Bidirectional Viterbi Algorithm (BVA), a suboptimal tail-biting decoder. The ‘Actual’ word-error performance of the suboptimal ‘BVA’ is slightly worse than that of the ML ‘Exact TB ROVA’. However, even though the bidirectional Viterbi decoder may choose a codeword other than the ML codeword, the posterior probability $P(\hat{x}^L|y^L)$ computed by PRC is exact. Thus, PRC provides reliability information about the decoded word that the receiver can use as retransmission criteria in a hybrid ARQ setting.

Fig. 7 also shows the performance of the combined TB SEA + ROVA(\hat{s}) approach in comparison with the exact TB ROVA. As shown in Thm. 1, the word-error probability calculated by the computationally efficient TB SEA + ROVA(s) is identical to that of TB ROVA, except when the probability of error is extremely high (i.e., when $P(\hat{x}|y) < \frac{1}{2}$). Even in the high-error regime, however, the difference is negligible.

Fig. 8 compares the exact and approximate versions of TB ROVA. For each starting state s , the ‘Exact TB ROVA’ uses Raghavan and Baum’s ROVA [1] and the ‘Approx TB ROVA’ uses Fricke and Hoehner’s simplified ROVA [4], as

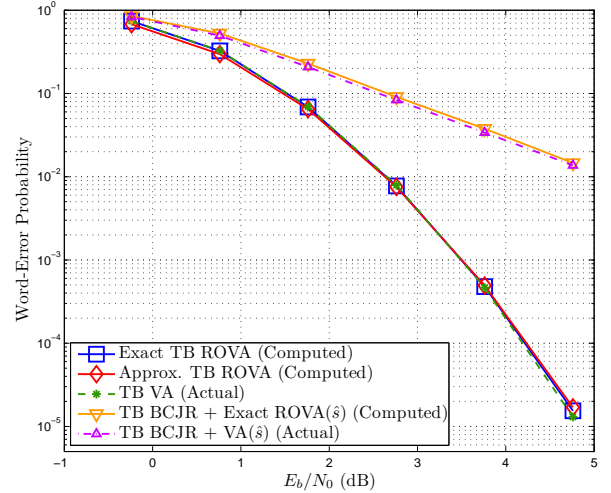


Fig. 8. Computed and actual word-error probability for the exact and approximate versions of TB ROVA (i.e., running ROVA(s) for each state s) on the AWGN channel. All simulations use the rate-1/3, 64-state convolutional code listed in Table II with $L = 128$ input bits and 384 output bits. The ‘Computed’ values are the word-error probabilities calculated by the receiver (averaged over the simulation) and the ‘Actual’ values count the number of words decoded incorrectly. The ‘TB BCJR’ method of estimating the initial state is shown for comparison, indicating that there is a severe penalty for disregarding the tail-biting restriction.

described in Sec. V. The approximate approach results in an estimated word-error probability that is very close to the exact word-error probability. Both reliability computations invoke the same decoder, the tail-biting Viterbi algorithm (‘TB VA’), so the ‘Actual’ curves are identical.

Fig. 8 also shows that when the forward recursion of the ‘TB BCJR’ of [12] is used to estimate the starting/ending state, there is a severe word-error penalty for disregarding the tail-biting restriction, as discussed in Sec. VI. The ‘TB BCJR’ simulations used one iteration through $L = 128$ trellis segments. Simulations with additional loops around the circular trellis did not improve the actual word-error probability, since the tail-biting condition was not enforced. Care should be taken when estimating the starting-state probability $P(s|y^L)$ based on observations of y^L in multiple trellis-loops.

Fig. 9 provides a histogram of the word-error probabilities computed by the receiver for the rate-1/3, 64-state convolutional code listed in Table II, with $L = 32$ input bits, 96 output bits and SNR 0 dB ($E_b/N_0 = 1.76$ dB). Fig. 9 illustrates that the exact and approximate TB ROVA approaches give very similar word-error probabilities, whereas the word-error probabilities computed by the tail-biting BCJR followed by ROVA(\hat{s}) differ significantly. The difference in the histogram for the TB BCJR is due to poorer decoder performance. Frequent errors in the state-estimation portion of the tail-biting BCJR cause the word-error probability to be high.

IX. ROVA FOR BLOCK CODES

Wolf [27] showed that the Viterbi algorithm could be applied to trellis representations of linear block codes, resulting in maximum-likelihood decoding. This section extends Raghavan and Baum’s ROVA [1] to linear block codes. Computing

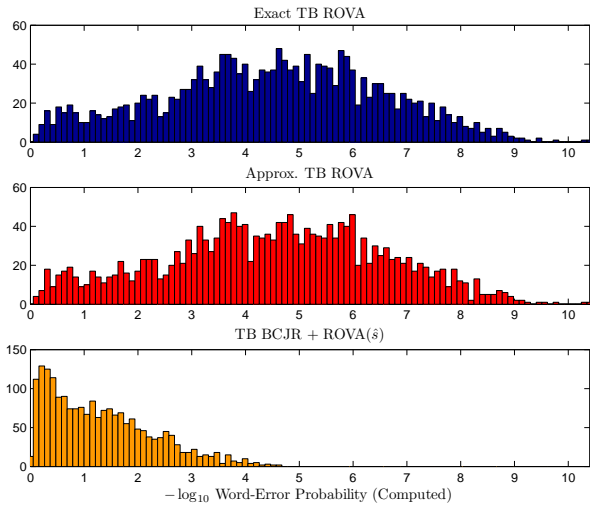


Fig. 9. Histograms of the word-error probability, plotted on a logarithmic scale, computed by three reliability-output decoders: TB ROVA with ML decoding and exact reliability computations, Approx TB ROVA with ML decoding and approximate reliability computations, and the TB BCJR for sub-optimal estimation of the starting state \hat{s} followed by ROVA(\hat{s}). Each histogram includes simulations of the same 2000 transmitted codewords and noise realizations. The two ML decoders compute $P(\hat{x}^L|y^L)$ for the same decoded word \hat{x}^L , whereas the suboptimal BCJR-based decoder decodes to a codeword that is not necessarily the same as \hat{x}^L . All simulations use the rate-1/3, 64-state convolutional code listed in Table II, with $L = 32$ input bits, 96 output bits and SNR 0 dB ($E_b/N_0 = 1.76$ dB).

the posterior probability $P(\hat{x}|y)$ of the decoded word \hat{x} with this version of the ROVA will enable the use of block codes in reliability-based retransmission schemes. Though terminated convolutional codes and tail-biting codes can both be thought of as block codes, in this section we will focus on block codes defined by a parity-check matrix H , where the entries in H are elements of $GF(q)$.

As with convolutional codes, each path in the trellis representation of a block code corresponds to a unique codeword. However, for an (n, k) block code, the number of states in the trellis at each trellis segment varies. Block codes start and end in the all-zeros state, and have a maximum of q^{n-k} states in the middle of the trellis.

The path-correct probabilities can again be computed recursively. Using the notation of [1], we define the following events:

- $p_j^\ell = \{\text{the survivor path from its beginning at state 0 to its arrival at state } j \text{ in segment } \ell \text{ is correct}\}$
- $\bar{p}_j^\ell = \{\text{one non-surviving path from its beginning at state 0 to its arrival at state } j \text{ in segment } \ell \text{ is correct}\}$
- $b_{ij}^\ell = \{\text{the branch from state } i \text{ to state } j \text{ at time } \ell \text{ is correct}\}$

The survivor path-correct probability at state j of trellis segment ℓ , $P(p_j^\ell|y^\ell)$, is the same as in (22):

$$P(p_j^\ell|y^\ell) = \frac{1}{\Delta_\ell} f(y_\ell|b_{ij}^\ell) P(p_i^{\ell-1}|y^{\ell-1}). \quad (31)$$

However, since all codewords start in the all-zeros state, we don't need to keep track of the events $\bar{p}_j^\ell(s) \forall s$, which we did for PRC and TB SEA. Instead, we are concerned only with

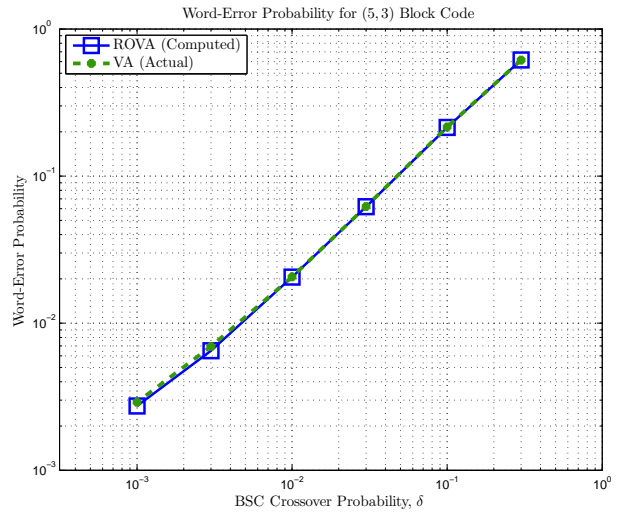


Fig. 10. Application of the ROVA to a trellis-decoded $(5, 3)$ block code from Wolf [27]. The actual word-error probability from the Viterbi algorithm (VA) matches the average of the word-error probabilities computed by the ROVA for each decoded word.

the event \bar{p}_j^ℓ . This probability of this event is:

$$P(\bar{p}_j^\ell|y^\ell) = \frac{1}{\Delta_\ell} \left(f(y_\ell|b_{ij}^\ell) P(\bar{p}_i^{\ell-1}|y^{\ell-1}) + \sum_{m \neq i: (m,j) \in \mathcal{T}_\ell} f(y_\ell|b_{mj}^\ell) [P(p_m^{\ell-1}|y^{\ell-1}) + P(\bar{p}_m^{\ell-1}|y^{\ell-1})] \right). \quad (32)$$

The sum in (32) is over all branches of the trellis \mathcal{T}_ℓ in segment ℓ that end in state j , except for the survivor branch (i, j) . The normalization constant of segment ℓ is

$$\Delta_\ell = \sum_{(m,r) \in \mathcal{T}_\ell} f(y_\ell|b_{mr}^\ell) [P(p_m^{\ell-1}|y^{\ell-1}) + P(\bar{p}_m^{\ell-1}|y^{\ell-1})]. \quad (33)$$

The sum in (33) is over all branches of the trellis \mathcal{T}_ℓ in segment ℓ .

The recursive computations in (31) and (32) continue until reaching the all-zeros state at the end of the n -segment trellis. At this point, (31) yields the quantity $1 - P(p_0^n|y^n) = 1 - P(\hat{x}^n|y^n) = P(\text{decoded word is in error})$. The complexity of the ROVA for block codes has order q^{n-k} , which is the maximum number of states in any segment of the trellis.

We demonstrate the application of the ROVA to the $(5, 3)$ binary block code given by Wolf [27]. The parity-check matrix H is

$$H = \begin{bmatrix} 1 & 1 & 0 & 1 & 0 \\ 1 & 0 & 1 & 0 & 1 \end{bmatrix}. \quad (34)$$

Fig. 10 confirms that the word-error probability computed by the ROVA matches the actual word-error probability obtained by Monte Carlo simulation. The $(5, 3)$ block code was simulated with transmission over the BSC with crossover probabilities ranging from 0.001 to 0.3. For binary codes over

the BSC with crossover probability δ , the conditional density $f(y_\ell|b_{i,j}^\ell)$ can be expressed as

$$f(y_\ell|b_{i,j}^\ell) = \delta^{d_H(y_\ell, x_\ell)}(1 - \delta)^{1-d_H(y_\ell, x_\ell)}, \quad (35)$$

where $d_H(y_\ell, x_\ell)$ is the Hamming distance between received symbol y_ℓ and encoder output symbol x_ℓ corresponding to the branch from state i to state j .

X. CONCLUSION

We have extended the reliability-output Viterbi algorithm to accommodate tail-biting codes, providing several types of tail-biting reliability-output decoders. TB ROVA invokes Raghavan and Baum's ROVA for each possible starting state s , and then computes the posterior probability of the ML starting state, $P(\hat{s}|y)$, in order to compute the overall word-error probability. We then demonstrated an approximate version of TB ROVA using Fricke and Hoehner's simplified ROVA. We introduced the Post-decoding Reliability Computation, which calculates the word-error probability of a decoded word, and the Tail-Biting State-Estimation Algorithm, which first computes the ML starting state \hat{s} and then decodes based on that starting state with ROVA(\hat{s}). Finally, we demonstrated that the ROVA can be applied to trellis representations of block codes.

A complexity analysis showed that TB SEA followed by ROVA(\hat{s}) reduces the number of operations by approximately half compared to TB ROVA. Importantly, Theorem 1 proved that the word-error probability computed by TB SEA + ROVA(\hat{s}) is the same as that computed by TB ROVA in SNR ranges of practical interest. Because of this, TB SEA is the recommended tail-biting decoder to use in reliability-based retransmission schemes (i.e., hybrid ARQ).

REFERENCES

- [1] A. Raghavan and C. Baum, "A reliability output Viterbi algorithm with applications to hybrid ARQ," *IEEE Trans. Inf. Theory*, vol. 44, no. 3, pp. 1214–1216, May 1998.
- [2] H. Ma and J. Wolf, "On tail biting convolutional codes," *IEEE Trans. Commun.*, vol. 34, no. 2, pp. 104–111, Feb. 1986.
- [3] S. Lin and D. J. Costello, *Error Control Coding, Second Edition*. Upper Saddle River, NJ, USA: Prentice-Hall, Inc., 2004.
- [4] J. Fricke and P. Hoehner, "Word error probability estimation by means of a modified Viterbi decoder," in *Proc. 66th IEEE Veh. Technol. Conf. (VTC)*, Oct. 2007, pp. 1113–1116.
- [5] H. Yamamoto and K. Itoh, "Viterbi decoding algorithm for convolutional codes with repeat request," *IEEE Trans. Inf. Theory*, vol. 26, no. 5, pp. 540–547, Sep. 1980.
- [6] J. Fricke and P. Hoehner, "Reliability-based retransmission criteria for hybrid ARQ," *IEEE Trans. Commun.*, vol. 57, no. 8, pp. 2181–2184, Aug. 2009.
- [7] E. Hof, I. Sason, and S. Shamai (Shitz), "On optimal erasure and list decoding schemes of convolutional codes," in *Proc. Tenth Int. Symp. Commun. Theory and Applications (ISCTA)*, July 2009, pp. 6–10.
- [8] G. Forney, "Exponential error bounds for erasure, list, and decision feedback schemes," *IEEE Trans. Inf. Theory*, vol. 14, no. 2, pp. 206–220, Mar. 1968.
- [9] A. R. Williamson, T.-Y. Chen, and R. D. Wesel, "Reliability-based error detection for feedback communication with low latency," in *Proc. 2013 IEEE Int. Symp. Inf. Theory (ISIT)*, Istanbul, Turkey, July 2013.
- [10] Y. Polyanskiy, H. V. Poor, and S. Verdú, "Channel coding rate in the finite blocklength regime," *IEEE Trans. Inf. Theory*, vol. 56, no. 5, pp. 2307–2359, May 2010.
- [11] —, "Feedback in the non-asymptotic regime," *IEEE Trans. Inf. Theory*, vol. 57, no. 8, pp. 4903–4925, Aug. 2011.
- [12] J. B. Anderson and S. M. Hladik, "Tailbiting MAP decoders," *IEEE J. Sel. Areas Commun.*, vol. 16, no. 2, pp. 297–302, Feb. 1998.
- [13] L. Bahl, J. Cocke, F. Jelinek, and J. Raviv, "Optimal decoding of linear codes for minimizing symbol error rate," *IEEE Trans. Inf. Theory*, vol. 20, no. 2, pp. 284–287, Mar. 1974.
- [14] J. B. Anderson and K. E. Tepe, "Properties of the tailbiting BCJR decoder," in *Codes, Systems, and Graphical Models*, B. Marcus and J. Rosenthal, Eds. New York: Springer-Verlag, 2001, pp. 211–238.
- [15] J. B. Anderson and S. M. Hladik, "An optimal circular Viterbi decoder for the bounded distance criterion," *IEEE Trans. Commun.*, vol. 50, no. 11, pp. 1736–1742, Nov. 2002.
- [16] R. Johannesson and K. Zigangirov, *Fundamentals of convolutional coding*. Piscataway, NJ, USA: IEEE Press, 1999.
- [17] M. Handlery, R. Johannesson, and V. Zyablov, "Boosting the error performance of suboptimal tailbiting decoders," *IEEE Trans. Commun.*, vol. 51, no. 9, pp. 1485–1491, Sep. 2003.
- [18] N. Y. Yu, "Performances of punctured tail-biting convolutional codes using initial state estimation," in *Proc. 68th IEEE Veh. Technol. Conf. (VTC)*, Sep. 2008, pp. 1–5.
- [19] R. Cox and C.-E. W. Sundberg, "An efficient adaptive circular Viterbi algorithm for decoding generalized tailbiting convolutional codes," *IEEE Trans. Veh. Technol.*, vol. 43, no. 1, pp. 57–68, Feb. 1994.
- [20] T.-Y. Wu, P.-N. Chen, H.-T. Pai, Y. S. Han, and S.-L. Shieh, "Reliability-based decoding for convolutional tail-biting codes," in *Proc. 71st IEEE Veh. Technol. Conf. (VTC)*, May 2010.
- [21] R. Y. Shao, S. Lin, and M. P. C. Fossorier, "Two decoding algorithms for tailbiting codes," *IEEE Trans. Commun.*, vol. 51, no. 10, pp. 1658–1665, Oct. 2003.
- [22] H.-T. Pai, Y. S. Han, and Y.-J. Chu, "New HARQ scheme based on decoding of tail-biting convolutional codes in IEEE 802.16e," *IEEE Trans. Veh. Technol.*, vol. 60, no. 3, pp. 912–918, Mar. 2011.
- [23] P. Shankar, P. N. A. Kumar, K. Sasidharan, and B. Rajan, "ML decoding of block codes on their tailbiting trellises," in *Proc. 2001 IEEE Int. Symp. Inf. Theory (ISIT)*, Washington, DC, June 2001, p. 291.
- [24] P. Shankar, P. N. A. Kumar, K. Sasidharan, B. S. Rajan, and A. S. Madhu, "Efficient convergent maximum likelihood decoding on tail-biting trellises," 2006. Available: <http://arxiv.org/abs/cs/0601023>.
- [25] J. Ortín, P. García, F. Gutiérrez, and A. Valdovinos, "A* based algorithm for reduced complexity ML decoding of tailbiting codes," *IEEE Commun. Lett.*, vol. 14, no. 9, pp. 854–856, Sep. 2010.
- [26] J. Anderson and K. Balachandran, "Decision depths of convolutional codes," *IEEE Trans. Inf. Theory*, vol. 35, no. 2, pp. 455–459, Mar. 1989.
- [27] J. Wolf, "Efficient maximum likelihood decoding of linear block codes using a trellis," *IEEE Trans. Inf. Theory*, vol. 24, no. 1, pp. 76–80, Jan. 1978.